ACS Macro Letters

Viewpoint

Cite This: ACS Macro Lett. 2018, 7, 968−975

pubs.acs.org/macroletters

Optical Tweezers Microrheology: From the Basics to Advanced Techniques and Applications

Rae M. Robertson-Anderson*

University of San Diego, Physics and Biophysics Department, 5998 Alcala Park, San Diego, California 92110, United States

ABSTRACT: Over the past few decades, microrheology has emerged as a widely used technique to measure the mechanical properties of soft viscoelastic materials. Optical tweezers offer a powerful platform for performing microrheology measurements and can measure rheological properties at the level of single molecules out to near macroscopic scales. Unlike passive microrheology methods, which use diffusing microspheres to extract rheological properties, optical tweezers can probe the nonlinear viscoelastic response, and measure the space- and time-dependent rheological properties of heterogeneous, non-equilibrium materials. In this Viewpoint, I describe the basic principles underlying optical tweezers microrheology, the instrumentation and material requirements, and key applications to widely studied soft biological materials. I also describe several sophisticated approaches that include coupling optical tweezers to fluorescence microscopy and microfluidics. The described techniques can robustly characterize noncontinuum mechanics, nonlinear mechanical responses, strain-field heterogeneities, stress propagation, force relaxation dynamics, and time-dependent mechanics of active materials.

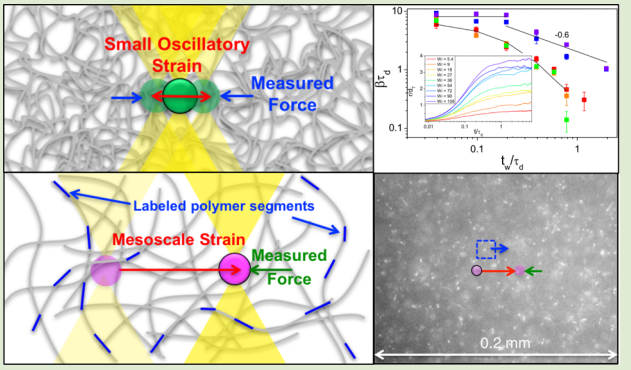

Optical tweezers, pioneered by Ashkin and co-workers in the 1970s,[1−3] have proven invaluable to elucidating important biological questions by enabling manipulation and high-resolution mechanical measurements of single molecules. For example, optical tweezers measurements have quantified the kinetics of kinesin walking along microtubules, the stretching profile of DNA, and the binding strength of actin to cross-linking proteins.[4−8] However, the ability to measure piconewton-level forces, and control and move micron-sized particles with nanometer precision, also make optical tweezers an exceptional platform for investigating the complex microscale rheology of macromolecular networks, soft materials, and non-Newtonian fluids.[9,10]

Rheology, the study of the flow and deformation of matter subject to applied forces, has been used extensively to shed light onto the complex mechanical properties of soft matter systems. These materials, which range from cytoplasm to ketchup, exhibit viscoelasticity, such that their response to strain cannot solely be described by fluid-like viscosity or solid-like elasticity. The rheological properties of these materials have traditionally been studied using bulk techniques in which the entire sample is strained and the bulk stress response is measured. However, many soft materials exhibit heterogeneities and scale-dependent rheology which bulk methods cannot discern.[11−14] Further, bulk rheometers often require ∼mL quantities, which limits their use for expensive or difficult to produce materials such as many biological systems.

To overcome these issues, researchers developed microrheology methods to measure microscale viscoelastic properties of soft materials using ∼μL volumes.[15−17] The most widely used technique is passive microrheology in which the trajectories of diffusing microspheres embedded in the material are tracked and used to extract the frequency-dependent elastic modulus $G'(\omega)$ and viscous modulus $G''(\omega)$. This method relies on generalized Stokes−Einstein relations to connect microbead trajectories to viscoelastic properties[16] and is limited to measuring linear response characteristics. Tracking single beads determines the rheological properties at the scale of the bead size (∼0.1−1 μm), which can be quite different than mesoscale and macroscale properties.[18−21] Two-point microrheology, which examines correlations between bead pairs,[14,21,22] can extract near-macroscopic moduli, but is inherently noisy and can be difficult to discern reliable, statistically significant signals.

Active microrheology, in which a microsphere is externally driven through a material, while the mechanical response to the strain is measured, offers an alternative to passive techniques and can provide enhanced capabilities and a wider parameter space of rheological deliverables. Optical tweezers allow for precision active microrheology measurements in which the velocity and displacement of the trapped bead are controlled with nanometer and millisecond precision and the resulting force is measured with subpiconewton accuracy. Optical tweezers are also highly adaptable and modular, enabling a wide range of added functionalities to be

Received: July 5, 2018
Accepted: July 20, 2018

DOI: 10.1021/acsmacrolett.8b00498
ACS Macro Lett. 2018, 7, 968−975

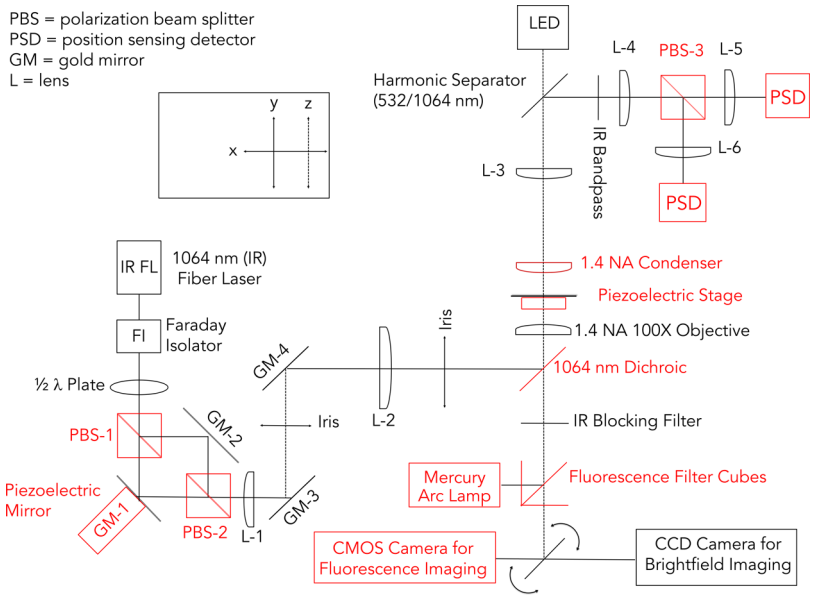

Figure 1. Schematic of optical trap with components needed for microrheology experiments. Components highlighted in red are those referred to in the text. Back focal plane force detection is achieved via a condenser and position sensing detector (PSD). Precision movement of the trap relative to the sample is achieved via a piezoelectric stage and/or mirror (GM-1). The mercury arc lamp, fluorescence filter cubes, 1064 nm dichroic, and CMOS camera are needed for fluorescence imaging. The polarization beam splitters (PBS), the second mirror (GM-2), and second PSD are needed for two traps. The remaining components are standard for optical tweezers.

incorporated into the instrument to allow for novel measurement techniques and the study of diverse material systems.

Instrumentation design and requirements: There are many excellent reviews on the basics of building and calibrating force-measuring optical tweezers.[23−28] I will focus on the instrumentation required for microrheology experiments (Figure 1).

For any microrheology experiment it is critical that the optical trap have back focal plane force detection,[26,28] as well as a fast (>10 kHz) data acquisition rate. Two-axis silicon-based position sensing diodes (PSD; e.g., First Sensors DL100−7 PCBA3) are well-suited for this need as they allow for two-dimensional measurements of laser deflection and can be easily configured to a data acquisition board for 100 kHz read rates. An objective with a high numerical aperture (NA ≥ 60×) is also ideal to ensure a strong trap that can withstand high resistive forces. However, the short working distance of high NA objectives can lead to hydrodynamic interactions with the sample boundary that can affect the apparent forces on the trapped particle.[29] To avoid these issues, No. 0 or 1 cover glasses are recommended.

Another important functionality is the ability to move the trapped bead relative to the sample at fast rates (∼100 Hz) with nanometer-scale precision and ∼ms response times. A two-axis piezoelectric stage (e.g., Mad City Laboratories Nano-PDQ250) that moves the sample (while keeping the trap fixed) meets these demands and allows for the bead to be moved in two dimensions to probe potential spatial asymmetries. An alternative approach is to use a piezoelectric mirror (e.g., Physik Instrumente S-330.8SD) to move the trap while keeping the sample fixed in space. The benefit of this approach is that the sample stays fixed so one can image the material during strain. The potential complication is that the movement of the trap will cause movement of the trapping beam that could be mistaken for force-induced laser deflection if the detection optics are not conjugate with the back focal plane of the objective.

While many microrheology experiments can be performed using bright-field microscopy (standard in all optical tweezers) to image beads, most biopolymers or macromolecules comprising soft materials are transparent to white light. Thus, to image macromolecular constituents during measurements it is advantageous to label them with fluorescent dyes and couple the optical trap to a fluorescence microscope. This can be done using an inverted fluorescence microscope (e.g., Olympus IX73) with an extra filter cube port stacked above the fluorescence filter cube turret. This extra port houses the dichroic filter for the trapping laser while the turret below houses the filters needed for fluorescence excitation and imaging.

To enable microrheology experiments such as those in references 30−34, one needs two spatially parallel optical traps. Two traps can be formed from a single laser by incorporating polarization beam splitters (PBS) into the light path to split the laser into horizontally and vertically polarized beams that each form a different trap. If one trap is controlled with a piezoelectric mirror then the two traps can be moved relative to each other. The force exerted on each trap can be separately measured by incorporating a second PSD and another beam splitter to separate the two polarizations after passing through the condenser. Finally, a digitally controlled laser shutter can be used to turn the laser on and off at precise time points to allow for experiments described in references 35 and 36.

Another important consideration is bead size and surface modification. Most systems of interest are not continuum materials but are instead networks of macromolecules with characteristic mesh or pore sizes. To measure the properties of the system rather than the pervading buffer the bead should be at least ∼3× larger than the system mesh size.[19,22] To ensure that the beads do not bind to (nonspecifically) or otherwise chemically interact with the material, they should be coated

DOI: 10.1021/acsmacrolett.8b00498
ACS Macro Lett. 2018, 7, 968−975

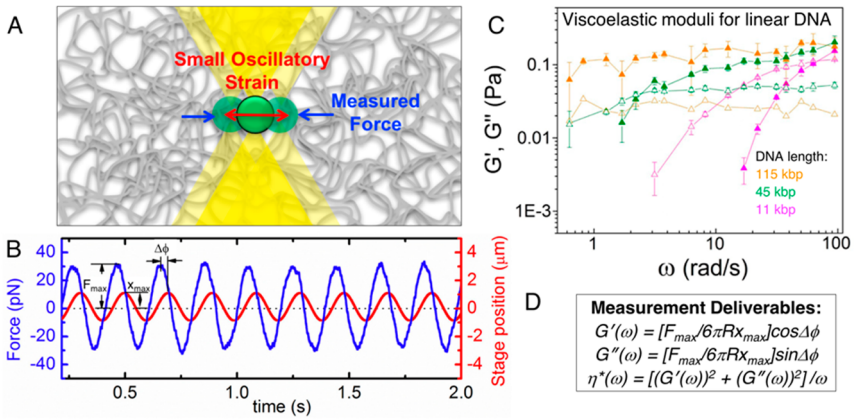

Figure 2. Linear oscillatory microrheology. (A) An optically trapped microsphere is sinusoidally displaced through the sample while the force exerted on the bead is measured. (B) Sample data showing the position of the stage (which moves the trap relative to the sample) and the measured force during oscillation. The stage amplitude x_{max}, force amplitude F_{max}, and phase shift $\Delta\phi$ between the two curves for each frequency ω are measured to compute the linear viscoelastic moduli. (C) $G'(\omega)$ (closed symbols) and $G''(\omega)$ (open symbols) measured using this method for 1 mg/mL linear DNA of varying lengths (listed in legend). Data is reproduced with permission from ref 19. Copyright 2014 ACS. (D) Equations relating measured quantities to viscoelastic moduli for a microsphere of a given radius R.

with small, noninteracting, neutral proteins or polymers such as BSA or PEG.[11,37,38] Carboxylated polystyrene beads (e.g., Polysciences, 17140−5) can be easily coated using carbodiimide cross-linking chemistry.[39] One can also incorporate fluorescent BSA (e.g., Alexa-488-BSA) into the reaction to enable simultaneous visualization of the bead and the fluorescent-labeled sample.[37]

Aqueous materials are best for manipulation of beads and straightforward force calibration. Systems that have been studied most widely using optical tweezers microrheology are networks of biopolymers such as DNA, wormlike micelles, and cytoskeleton filaments, as well mucus and systems of synthetic polymers.[11,13,35,36,40−44] These systems have rich viscoelastic behavior but the volume fraction of biopolymers is low enough such that the materials are primarily comprised of water.

For most techniques, multiple individual trials should be executed, each taken with a different bead in a different location in the sample chamber. While most post-acquisition analyses are performed using the average of all trials, rich information can be obtained from the distribution of individual measurements which should be carefully examined.[13,45] This distribution can bear evidence of spatial heterogeneities, phase separation, and molecular individuality, as well as macromolecular buckling and rupturing events.[13] In fact, one of the advantages of active microrheology over other techniques is the ability to perform localized measurements throughout the material and resolve length scales over which heterogeneities are present.[11−13,19]

Standard measurement techniques: The most basic active microrheology technique, analogous to conventional bulk linear rheology measurements, is to sinusoidally oscillate a trapped bead with small amplitudes x_{max} and a wide range of frequencies ω (Figure 2).[19,40,46] By measuring the resulting force F during oscillations and comparing to the measured trap displacement x, one can determine the frequency-dependent elastic modulus $G'(\omega)$, viscous modulus $G''(\omega)$, and complex viscosity $\eta^*(\omega)$. Specifically, from the oscillation amplitudes of the force F_{max} and trap position x_{max}, and the phase shift between the two sine curves $\Delta\phi$, one can compute the viscoelastic moduli as $G'(\omega) = [F_{max}/6\pi Rx_{max}]\cos\Delta\phi$, $G''(\omega) = [F_{max}/6\pi Rx_{max}]\sin\Delta\phi$ and $\eta^*(\omega) = [(G'(\omega))^2 + (G''(\omega))^2]^{1/2}/\omega$ (Figure 2D). For these measurements, the amplitude should be chosen to be large enough to measure an appreciable signal for low frequencies but small enough to be in the linear amplitude-independent regime.

This technique has been used to characterize the viscoelastic properties of networks of DNA, actin, intermediate filaments, and mucus and has shown that these systems exhibit hierarchical and anisotropic structure and mechanical response at the microscale.[11,12,19,46] For example, studies on entangled DNA showed that the noncontinuum characteristics of the network play an important role in the measured response until the bead diameter exceeds ∼3× the entanglement tube diameter d_T.[19]

To perturb a material far from equilibrium, and determine how the mechanical response depends on the length scale of the strain, largescale constant speed strains can be performed. These measurements also allow for measuring mesoscale viscoelastic properties, inaccessible to passive microrheology and bulk macrorheology. In this technique, the bead is moved at a constant speed v over a displacement x that is large compared to the intrinsic length scales of the system, while the force F is measured as a function of x (Figure 3). These measurements are analogous to nonlinear rheology measurements that apply a strain γ with a constant strain rate $\dot{\gamma}$ and measure the dependence of stress σ on γ and $\dot{\gamma}$. To directly compare results to those of macrorheology measurements, displacement, speed, and force can be converted to strain, strain rate, and stress using the following relations: $\gamma = x/2R$, $\dot{\gamma} = 3v/\sqrt{2}R$, $\sigma = F/\pi R^2$.[36,47] From $F(x)$ one can also determine an effective differential modulus, which quantifies the system elasticity or stiffness, by computing the derivative of F with respect to x or γ: $K(x) = dF(x)/dx$ or $K(\gamma) = d\sigma(\gamma)/d\gamma$ (Figure 3D,E). For materials that exhibit a viscous steady-state response, in which $F(x)$ reaches an x-independent plateau at large distances, these measurements can be used to determine the steady-state viscosity $\eta(\dot{\gamma})$ and its dependence on strain rate.[36,44]

Typical distances used in these measurements are ∼10−30 μm, with the upper bound limited by the range of the piezoelectric stage and the linearity of the trap at large bead deflections. Speeds typically vary from ∼1−10^2 μm/s depend-

DOI: 10.1021/acsmacrolett.8b00498
ACS Macro Lett. 2018, 7, 968−975

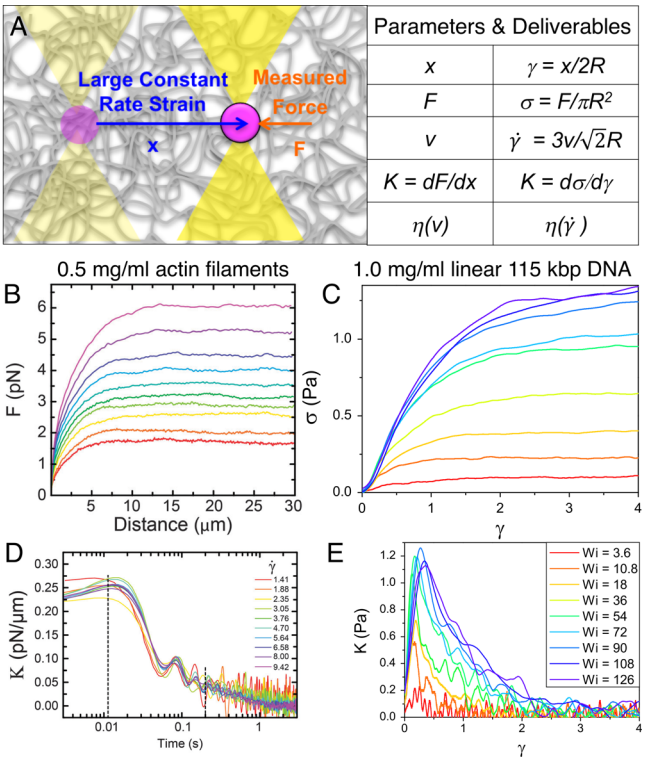

Figure 3. Nonlinear mesoscale microrheology. (A) A trapped bead is moved at a constant speed v over a large distance x as the force F the sample exerts on the bead is measured. An effective differential modulus $K = dF/dx$ and viscosity η can be determined from the measured $F(x)$ curves (table column 1). All quantities for a given bead radius R can be converted to those used in macrorheology (table column 2). (B–G) Data for entangled networks of actin (left) and DNA (right). (B, C) Force curves for varying strain rates (or Wi) as displayed in legends in D and E. (D) $K(x)$ determined from $F(x)$ curves in B. Dashed lines correspond to actin relaxation time scales. (E) $K(\gamma)$ determined from $\sigma(\gamma)$ curves in C. B–E are reproduced with permission from references 36 and 44. Copyright 2014 APS and Copyright 2015 RSC, respectively.

ing on the relaxation time scales of the system, the strength of the optical trap, and the response time of the stage. To access the nonlinear regime, speeds should be several times faster than the relaxation time of the material. In other words, the Weissenberg number Wi should be much greater than 1.[36] Slower speed measurements can identify the crossover point from linear to nonlinear rheological response.[36,44,54] However, care must be taken when interpreting the results of these nonlinear measurements, as discussed in references 47–50. Further, due to the different nature of the flow field compared to macrorheology experiments, a direct comparison between the two techniques cannot be done blindly. In fact, differences between results from micro- and macrorheology can shed important light onto the complex structure and nonlinear flow response of many viscoelastic materials.[37,51–53]

The time-dependent relaxation of strain-induced force can be measured following constant speed strains to determine stress relaxation profiles (Figure 4). The most straightforward method is to continue to measure the force exerted on the trapped bead once the strain has completed, resulting in time-dependent force decay curves (Figure 4A,B).[13,44,54,55] Most relaxation profiles of viscoelastic materials can be fit to a sum of exponentials ($F(t) \sim Ae^{-t/\tau_1} + Be^{-t/\tau_2} + ...$) if the relaxation time constants τ_N are well separated in time.[45,54] Inverse Laplace transform analysis can be used to determine the number of distinct decays present in the relaxation curves,[30] and exponential fits to the data can determine the corresponding relaxation time scales τ_N.[45,54] For heterogeneous systems or in the nonlinear regime, force decays often exhibit power-law decay $F(t) \sim t^{-\alpha}$, and the scaling exponents can be determined from the measured relaxation curves (Figure 4B).[13,36,44,55]

An alternative method for analyzing relaxation dynamics is to shut the laser off after the strain completes and track the recoil of the released bead (Figure 4C,D).[35,36] The bead displacement can be tracked using high frame-rate video capture. Bead trajectories, maximum recoil distances and time scales over which recoil takes place can be analyzed to quantify the relative viscous and elastic contributions to the relaxation, and the mesh size or entanglement length of macromolecular networks.[36] By varying the "wait times" t_w following the strain before the laser is shut off, one can quantify the time dependence of stress relaxation and the intrinsic relaxation time scales of the system (Figure 4D).

An alternative approach to the active methods described above is to use the Brownian motion of a trapped bead to extract viscoelastic properties. This method, which requires nothing more than an optical trap with force detection, is more akin to passive microrheology as there is no active forcing of the bead through the sample. In these measurements, generalized Stokes–Einstein relationships are used to relate the mean-squared displacement, position autocorrelation function, or power spectrum of the trapped bead to the linear viscoelastic moduli $G'(\omega)$ and $G''(\omega)$.[9,56] These techniques, as well as their applications, have been covered extensively elsewhere.[9,17,41,42,57,58]

Advanced approaches: The stress response of a material is often used to deduce the dynamics and interactions of the macromolecules comprising the system. However, few methods can directly couple the strain-induced deformations and motions of the macromolecular components with the resulting stress imposed in the material. One can achieve this goal by combining optical tweezers microrheology with fluorescence microscopy and particle-tracking (Figure 5).[37,45] In this technique, a fraction of the polymers comprising the system are fluorescent-labeled such that they can be tracked as point particles over time, and fast frame-rate videos are recorded during and after the strain applied by the trapped bead (Figure 5A,B).[37,45] For these measurements, the sample must remain fixed in the imaging plane, so to apply a strain, the trap itself must be moved (via a piezoelectric mirror, Figure 1). To determine how the network responds during strain, it is important that the camera frame rate be several times faster than the strain rate, so multiple frames can be acquired during the bead motion. This active particle-tracking method can extract all of the information from the methods described above while simultaneously measuring the distribution of particle velocities and trajectories at varying positions from the applied perturbation. Particle-tracking algorithms, such as those from Crocker and Weeks,[59] can be used to calculate particle trajectories, from which one can determine the maximum strain-induced displacements and velocities of the particles, as well as the subsequent recoil distances following the strain (Figure 5C). By analyzing the distributions of displacements and velocities for different radial distances from the strain site, one can map the strain field of the network and

DOI: 10.1021/acsmacrolett.8b00498
ACS Macro Lett. 2018, 7, 968–975

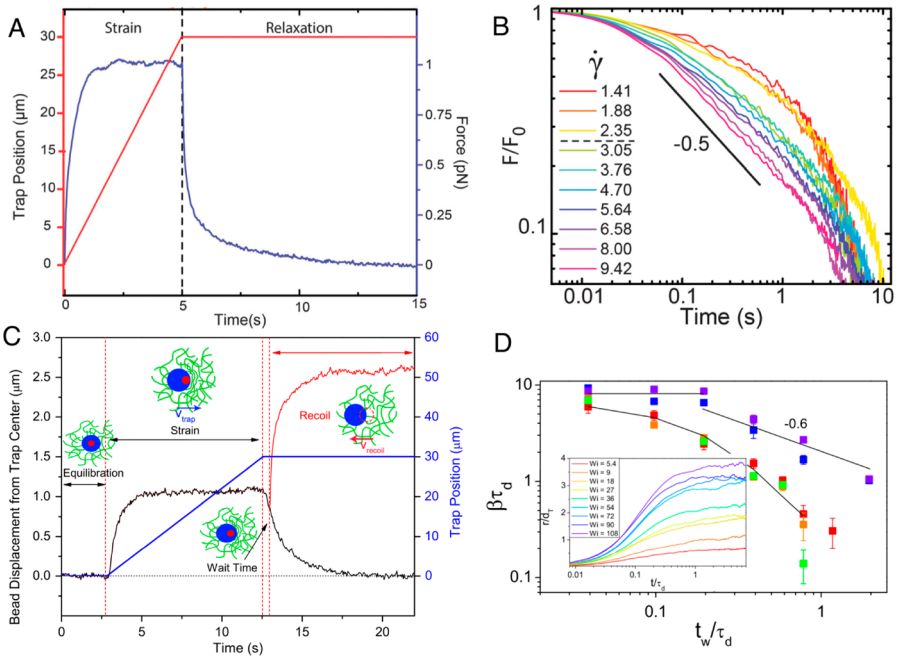

Figure 4. Measuring local stress relaxation following mesoscale strains. (A) Following trap displacement (red), the trap is held fixed and the relaxation of the force exerted on the trapped bead (blue) is measured over time. (B) Force relaxation for entangled actin (same system as Figure 3) for varying $\dot{\gamma}$ listed in legend. The force is normalized by the value at the beginning of relaxation F_0. The data show a crossover from exponential to power-law relaxation at a strain rate of ~3 s^{-1}. The black line represents power-law scaling with the exponent listed. (C) Following trap displacement (blue), the bead is held in the trap for a specific wait time t_w, after which the trap is turned off and the trajectory of the released bead is tracked (red). The force on the bead during strain, proportional to the bead displacement from the trap center (black), is recorded during Strain and Wait Time. (D) The decay rate β of the bead recoil as a function of wait time t_w for varying Wi (legend in inset and Figure 3E) for entangled DNA (same system as Figure 3). β, normalized by the disengagement rate τ_D^{-1} of the system, is determined by fitting each recoil trajectory r (inset) to a single exponential. Solid lines through $Wi > 20$ data are power-laws with exponents of 0 and −0.6. Solid line through $Wi < 20$ data is an exponential decay function. Inset: Recoil trajectories as a function of time t. Figures reproduced from references 44 and 36. Copyright 2015 RSC and Copyright 2014 APS, respectively.

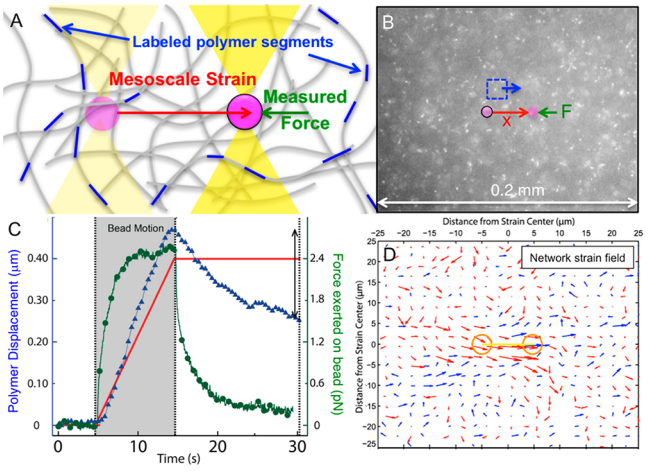

Figure 5. Active macromolecular-tracking microrheology couples mechanical response to polymer mobility. (A, B) An optically trapped microsphere is displaced a distance x (red) while the force F (green) exerted on the bead is measured before, during and following the strain. Concurrent with force measurements, mobility and deformations of single discretely labeled polymers (blue) are imaged and tracked. (C) Each measurement results in a force (green) and an average polymer velocity and displacement (blue) in varying regions of the network (blue box, B). (D) Spatially resolved polymer velocity vectors map the deformation field surrounding the strain to characterize stress propagation dynamics and length scales.

determine how stress propagates from the strain site and distributes through the network (Figure 5D). For this analysis, it is important that the strain path is centered in the field of view and that the field of view is several times larger than the length scale of the bead displacement (Figure 5B,D). References 37 and 45, which use this technique to investigate the nonlinear response of actin networks, describe in detail how to execute these measurements and the wealth of information that can be obtained.

To directly measure interaction forces between the constituents of a polymeric material and characterize their confinement, one can use the polymers themselves to impose strain and measure stress.[30,31] This technique requires the ends of the polymer (typically a biopolymer) to be functionalized to bind microspheres,[5,60] and two traps to hold the two bead "handles" of the polymer. For microrheology measurements, the biopolymer is stretched taught and moved in a direction transverse to its contour at a constant speed through the sample. The resulting force exerted on each bead handle during and following the displacement is measured. Control experiments in which only beads are trapped are also performed and the force profiles are subtracted from those in which a biopolymer is present to determine the force induced solely in the biopolymer. These measurements can be used to directly probe the transverse tube confinement potential in entangled polymer systems[30,31] and shed light on the interaction forces between polymers in a network. The force relaxation following displacement can resolve the system relaxation time scales and associated mechanisms. The extended range of the applied

DOI: 10.1021/acsmacrolett.8b00498
ACS Macro Lett. 2018, 7, 968−975

force can also more accurately detect hooking and slippage of polymers during displacement.[30,31] Further, two parallel optical traps can be used to perform other novel microrheology measurements.[32,34,33] For instance, tracking the motion of a bead as it flips between two traps that alternately shut on and off provide the low frequency viscoelastic response of a material.[32] Measuring the signal from a fixed trapped bead as an adjacent trapped bead is oscillated can be used to measure fluid viscosity and test the validity of the fluctuation−dissipation theorem.[33,34]

Many soft materials and macromolecular networks, particularly biological ones, are dynamic nonequilibrium systems that readily change their properties in response to changing chemical environments. For example, actin proteins polymerize and depolymerize depending on the concentration of $MgCl_2$, $CaCl_2$, and ATP in solution. Biological motors and enzymes alter the size and topology of DNA and induce morphological changes in cytoskeleton networks depending on the buffer conditions. To understand how chemically triggered activity alters the mechanical properties of active or driven systems, one requires a method to alter buffer conditions in situ while simultaneously measuring the time-varying mechanical properties of nonequilibrium materials. To enable these measurements optical tweezers microrheology can be coupled with microfluidic perfusion chambers.[61] In these measurements, the chemical environment is altered in real-time via microfluidics while small oscillation microrheology is performed in set time intervals to determine how the mechanical properties evolve and transition between different states (Figure 6).[62]

The microfluidic devices, based on methods from reference 61, are prepared using microscope slides, spacers and coverslips compatible with most optical tweezers setups. The devices have a central sample chamber bordered on top and bottom by semipermeable membranes and flanking buffer channels (Figure 6A). After loading the sample into the central chamber, the left and right sides of the chamber are sealed so the sample is completely enclosed. Tubing inserted into both ends of the buffer channels enables buffer exchange within the sample chamber via passive diffusion through the membranes. These strategically designed chambers can modulate the chemical environment of the system while preventing directional flow, disruption, or loss of sample. Microrheology measurements can be executed before, during and after buffer exchange to determine the effect of dynamic modulation of chemical environments on the mechanical properties of the material (Figure 6B,C).

Outlook: Optical tweezers microrheology is a powerful platform for elucidating the microscale and mesoscale mechanical properties of a wide range of macromolecular systems and soft materials. There are more optical tweezers microrheology methods than were covered here,[9,12,17,43,65] and new methods continue to be developed. Most applications to date, which have been referenced in the preceding sections, have been on networks of biopolymers including DNA, actin, microtubules, intermediate filaments, and wormlike micelles.[12,13,36,37,42,45] However, these techniques have also been applied to synthetic polymers, mucus, vitreous humor, and viscous fluids.[9,11,32,35,41,43]

While many technological advances have been made in the field of microrheology to enable the versatile measurements described above, theoretical models that predict microrheology data remain underdeveloped.[16,66,67] While the results of microrheology are often compared to those of macrorheology, the nature of the strain field in the two techniques are indeed different. Complete understanding of existing microrheology data, as well as future advances to the field, will rely on new theoretical models to be developed that can accurately describe the strain field induced by the moving microsphere, and its effects on the macromolecules comprising the myriad of soft matter systems investigated with this method.

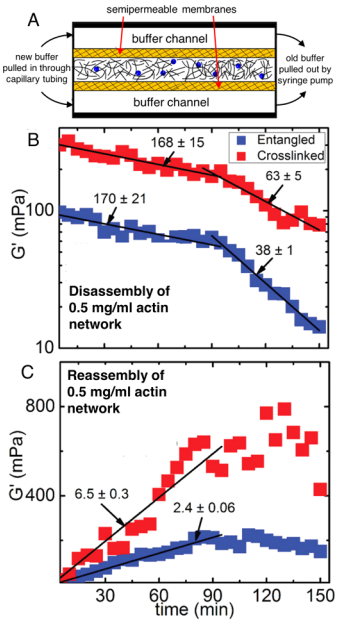

Figure 6. Time-resolved microrheology during triggered activity of nonequilibrium materials. (A) Microfluidic device used to change buffer conditions without mechanical disruption or loss of the sample. The cartoon shows actin filaments and microspheres sealed in the central sample chamber, flanked by membranes that are permeable to small molecules but not macromolecules.[62,63] Buffer channels connected to capillary tubing allow for existing buffer to be pulled out of the chamber while the desired buffer is pulled in. Prior to experiments, buffer channels are filled with the buffer that matches that of the sample. To change the chemical environment of the sample, a digitally controlled syringe pump pulls the existing buffer from the flanking channels while the new desired buffer is pulled in. The membrane thickness and flow rate are set so that the new buffer is able to diffuse into the sample chamber while the existing buffer diffuses out.[61,64] (B, C) Time-dependent elastic moduli $G'(\omega)$ of actin networks during depolymerization (disassembly, B) and subsequent repolymerization (reassembly, C) of actin filaments triggered by varying concentrations of $MgCl_2$, $CaCl_2$, and ATP. Red and blue curves are ω-averaged values for networks with (red) and without (blue) 2% biotin-NeutrAvidin crosslinkers. Solid black lines are (B) fits to single exponentials with time constants listed in min, and (C) linear fits with slopes listed in mPa-min^{-1}. Data is reproduced from reference 62.

AUTHOR INFORMATION

Corresponding Author

*E-mail: randerson@sandiego.edu.

ORCID

Rae M. Robertson-Anderson: 0000-0003-4475-4667

Notes

The author declares no competing financial interest.

DOI: 10.1021/acsmacrolett.8b00498
ACS Macro Lett. 2018, 7, 968−975

■ ACKNOWLEDGMENTS

This work was funded by an AFOSR Biomaterials Award (No. FA9550-17-1-0249) and an NSF CAREER Award (No. 1255446).

■ REFERENCES

(1) Ashkin, A. Acceleration and Trapping of Particles by Radiation Pressure. *Phys. Rev. Lett.* **1970**, *24* (4), 156−159.
(2) Ashkin, A.; Dziedzic, J. M. Optical Levitation by Radiation Pressure. *Appl. Phys. Lett.* **1971**, *19* (8), 283−285.
(3) Ashkin, A.; Dziedzic, J. M.; Bjorkholm, J. E.; Chu, S. Observation of a Single-Beam Gradient Force Optical Trap for Dielectric Particles. *Opt. Lett.* **1986**, *11* (5), 288−290.
(4) Bennink, M. L.; Leuba, S. H.; Leno, G. H.; Zlatanova, J.; Grooth, B. G.; de Greve, J. Unfolding Individual Nucleosomes by Stretching Single Chromatin Fibers with Optical Tweezers. *Nat. Struct. Biol.* **2001**, *8* (7), 606−610.
(5) Wang, M. D.; Yin, H.; Landick, R.; Gelles, J.; Block, S. M. Stretching DNA with Optical Tweezers. *Biophys. J.* **1997**, *72* (3), 1335−1346.
(6) Bianco, P.; Nagy, A.; Kengyel, A.; Szatmári, D.; Mártonfalvi, Z.; Huber, T.; Kellermayer, M. S. Z. Interaction Forces between F-Actin and Titin PEVK Domain Measured with Optical Tweezers. *Biophys. J.* **2007**, *93* (6), 2102−2109.
(7) Ferrer, J. M.; Lee, H.; Chen, J.; Pelz, B.; Nakamura, F.; Kamm, R. D.; Lang, M. J. Measuring Molecular Rupture Forces between Single Actin Filaments and Actin-Binding Proteins. *Proc. Natl. Acad. Sci. U. S. A.* **2008**, *105* (27), 9221−9226.
(8) *Force of single kinesin molecules measured with optical tweezers | Science* http://science.sciencemag.org/content/260/5105/232 (accessed Jun 21, 2018).
(9) Tassieri, M. *Microrheology with Optical Tweezers: Principles and Applications*; CRC Press, 2016.
(10) Furst, E. M.; Squires, T. M. *Microrheology*; Oxford University Press, 2017.
(11) Weigand, W. J.; Messmore, A.; Tu, J.; Morales-Sanz, A.; Blair, D. L.; Deheyn, D. D.; Urbach, J. S.; Robertson-Anderson, R. M. Active Microrheology Determines Scale-Dependent Material Properties of Chaetopterus Mucus. *PLoS One* **2017**, *12* (5), e0176732.
(12) Neckernuss, T.; Mertens, L. K.; Martin, I.; Paust, T.; Beil, M.; Marti, O. Active Microrheology with Optical Tweezers: A Versatile Tool to Investigate Anisotropies in Intermediate Filament Networks. *J. Phys. D: Appl. Phys.* **2016**, *49* (4), 045401.
(13) Ricketts, S. N.; Ross, J. L.; Robertson-Anderson, R. M. Co-Entangled Actin-Microtubule Composites Exhibit Tunable Stiffening and Power-Law Stress Relaxation. *bioRxiv* **2018**, na.
(14) Crocker, J. C.; Valentine, M. T.; Weeks, E. R.; Gisler, T.; Kaplan, P. D.; Yodh, A. G.; Weitz, D. A. Two-Point Microrheology of Inhomogeneous Soft Materials. *Phys. Rev. Lett.* **2000**, *85* (4), 888−891.
(15) Brau, R. R.; Ferrer, J. M.; Lee, H.; Castro, C. E.; Tam, B. K.; Tarsa, P. B.; Matsudaira, P.; Boyce, M. C.; Kamm, R. D.; Lang, M. J. Passive and Active Microrheology with Optical Tweezers. *J. Opt. A: Pure Appl. Opt.* **2007**, *9* (8), S103.
(16) Squires, T. M.; Mason, T. G. Fluid Mechanics of Microrheology. *Annu. Rev. Fluid Mech.* **2010**, *42* (1), 413−438.
(17) Waigh, T. A. Advances in the Microrheology of Complex Fluids. *Rep. Prog. Phys.* **2016**, *79* (7), 074601.
(18) Furst, E. M. Applications of Laser Tweezers in Complex Fluid Rheology. *Curr. Opin. Colloid Interface Sci.* **2005**, *10* (1), 79−86.
(19) Chapman, C. D.; Lee, K.; Henze, D.; Smith, D. E.; Robertson-Anderson, R. M. Onset of Non-Continuum Effects in Microrheology of Entangled Polymer Solutions. *Macromolecules* **2014**, *47* (3), 1181−1186.
(20) Gardel, M. L.; Valentine, M. T.; Crocker, J. C.; Bausch, A. R.; Weitz, D. A. Microrheology of Entangled F-Actin Solutions. *Phys. Rev. Lett.* **2003**, *91* (15), 158302.
(21) Liu, J.; Gardel, M. L.; Kroy, K.; Frey, E.; Hoffman, B. D.; Crocker, J. C.; Bausch, A. R.; Weitz, D. A. Microrheology Probes Length Scale Dependent Rheology. *Phys. Rev. Lett.* **2006**, *96* (11), 118104.
(22) Buchanan, M.; Atakhorrami, M.; Palierne, J. F.; Schmidt, C. F. Comparing Macrorheology and One- and Two-Point Microrheology in Wormlike Micelle Solutions. *Macromolecules* **2005**, *38* (21), 8840−8844.
(23) Fazal, F. M.; Block, S. M. *Optical tweezers study life under tension* https://www.nature.com/articles/nphoton.2011.100 (accessed Jun 21, 2018).
(24) Molloy, J. E.; Padgett, M. J. Lights, Action: Optical Tweezers. *Contemp. Phys.* **2002**, *43* (4), 241−258.
(25) Neuman, K. C.; Nagy, A. Single-Molecule Force Spectroscopy: Optical Tweezers, Magnetic Tweezers and Atomic Force Microscopy. *Nat. Methods* **2008**, *5* (6), 491−505.
(26) Tolić-Nørrelykke, S. F.; Schäffer, E.; Howard, J.; Pavone, F. S.; Jülicher, F.; Flyvbjerg, H. Calibration of Optical Tweezers with Positional Detection in the Back Focal Plane. *Rev. Sci. Instrum.* **2006**, *77* (10), 103101.
(27) Lang, M. J.; Block, S. M. Resource Letter: LBOT-1: Laser-Based Optical Tweezers. *Am. J. Phys.* **2003**, *71* (3), 201−215.
(28) Jones, P. H.; Maragò, O. M.; Volpe, G. *Optical Tweezers: Principles and Applications*; Cambridge University Press, 2015.
(29) Swan, J. W.; Furst, E. M. Nonequilibrium Distributions and Hydrodynamic Coupling Distort the Measurement of Nanoscale Forces near Interfaces. *Biophys. J.* **2013**, *104* (4), 863−872.
(30) Robertson, R. M.; Smith, D. E. Direct Measurement of the Intermolecular Forces Confining a Single Molecule in an Entangled Polymer Solution. *Phys. Rev. Lett.* **2007**, *99* (12), na.
(31) Robertson, R. M.; Smith, D. E. Direct Measurement of the Confining Forces Imposed on a Single Molecule in a Concentrated Solution of Circular Polymers. *Macromolecules* **2007**, *40* (24), 8737−8741.
(32) Preece, D.; Warren, R.; Evans, R. M. L.; Gibson, G. M.; Padgett, M. J.; Cooper, J. M. Manlio Tassieri. Optical Tweezers: Wideband Microrheology. *J. Opt.* **2011**, *13* (4), 044022.
(33) Paul, S.; Kumar, R.; Banerjee, A. Two-Point Active Microrheology in a Viscous Medium Exploiting a Motional Resonance Excited in Dual-Trap Optical Tweezers. *Phys. Rev. E: Stat. Phys., Plasmas, Fluids, Relat. Interdiscip. Top.* **2018**, *97* (4), na.
(34) Paul, S.; Laskar, A.; Singh, R.; Roy, B.; Adhikari, R.; Banerjee, A. Direct Verification of the Fluctuation-Dissipation Relation in Viscously Coupled Oscillators. *Phys. Rev. E: Stat. Phys., Plasmas, Fluids, Relat. Interdiscip. Top.* **2017**, *96* (5), 050102.
(35) Gomez-Solano, J. R.; Bechinger, C. Transient Dynamics of a Colloidal Particle Driven through a Viscoelastic Fluid. *New J. Phys.* **2015**, *17* (10), 103032.
(36) Chapman, C. D.; Robertson-Anderson, R. M. Nonlinear Microrheology Reveals Entanglement-Driven Molecular-Level Viscoelasticity of Concentrated DNA. *Phys. Rev. Lett.* **2014**, *113* (9), na.
(37) Falzone, T. T.; Robertson-Anderson, R. M. Active Entanglement-Tracking Microrheology Directly Couples Macromolecular Deformations to Nonlinear Microscale Force Response of Entangled Actin. *ACS Macro Lett.* **2015**, *4* (11), 1194−1199.
(38) Rapid transport of large polymeric nanoparticles in fresh undiluted human mucus | PNAS http://www.pnas.org/content/104/5/1482.short (accessed Jun 22, 2018).
(39) 238E-Adsorbing-Proteins-PS-Spheres.pdf.
(40) Valentine, M. T.; Dewalt, L. E.; Ou-Yang, H. D. Forces on a Colloidal Particle in a Polymer Solution: A Study Using Optical Tweezers. *J. Phys.: Condens. Matter* **1996**, *8* (47), 9477.
(41) Watts, F.; Tan, L. E.; Wilson, C. G.; Girkin, J. M.; Tassieri, M.; Wright, A. J. Investigating the Micro-Rheology of the Vitreous Humor Using an Optically Trapped Local Probe. *J. Opt.* **2014**, *16* (1), 015301.
(42) Morishima, K.; Inoue, T. High Frequency Viscoelastic Measurements Using Optical Tweezers on Wormlike Micelles of

DOI: 10.1021/acsmacrolett.8b00498
ACS Macro Lett. 2018, 7, 968−975

Nonionic and Cationic Surfactants in Aqueous Solutions. *J. Rheol.* **2016**, *60* (6), 1055−1067.
(43) Tassieri, M.; Giudice, F. D.; Robertson, E. J.; Jain, N.; Fries, B.; Wilson, R.; Glidle, A.; Greco, F.; Netti, P. A.; Maffettone, P. L.; Cooper, T. M. Microrheology with Optical Tweezers: Measuring the Relative Viscosity of Solutions 'at a Glance'. *Sci. Rep.* **2015**, *5*, 8831.
(44) Falzone, T. T.; Blair, S.; Robertson-Anderson, R. M. Entangled F-Actin Displays a Unique Crossover to Microscale Nonlinearity Dominated by Entanglement Segment Dynamics. *Soft Matter* **2015**, *11* (22), 4418−4423.
(45) Gurmessa, B.; Ricketts, S.; Robertson-Anderson, R. M. Nonlinear Actin Deformations Lead to Network Stiffening, Yielding, and Nonuniform Stress Propagation. *Biophys. J.* **2017**, *113* (7), 1540−1550.
(46) Lee, H.; Ferrer, J. M.; Nakamura, F.; Lang, M. J.; Kamm, R. D. Passive and Active Microrheology for Cross-Linked F-Actin Networks in Vitro. *Acta Biomater.* **2010**, *6* (4), 1207−1218.
(47) Squires, T. M. Nonlinear Microrheology: Bulk Stresses versus Direct Interactions. *Langmuir* **2008**, *24* (4), 1147−1159.
(48) DePuit, R. J.; Squires, T. M. Micro−Macro Discrepancies in Nonlinear Microrheology: II. Effect of Probe Shape. *J. Phys.: Condens. Matter* **2012**, *24* (46), 464107.
(49) DePuit, R. J.; Khair, A. S.; Squires, T. M. A Theoretical Bridge between Linear and Nonlinear Microrheology. *Phys. Fluids* **2011**, *23* (6), 063102.
(50) DePuit, R. J.; Squires, T. M. Micro−Macro-Discrepancies in Nonlinear Microrheology: I. Quantifying Mechanisms in a Suspension of Brownian Ellipsoids. *J. Phys.: Condens. Matter* **2012**, *24* (46), 464106.
(51) Sriram, I.; Furst, E. M.; DePuit, R. J.; Squires, T. M. Small Amplitude Active Oscillatory Microrheology of a Colloidal Suspension. *J. Rheol.* **2009**, *53* (2), 357−381.
(52) Cribb, J. A.; Vasquez, P. A.; Moore, P.; Norris, S.; Shah, S.; Forest, M. G. Superfine, R. Nonlinear Signatures in Active Microbead Rheology of Entangled Polymer Solutions. *J. Rheol.* **2013**, *57* (4), 1247−1264.
(53) Meyer, A.; Marshall, A.; Bush, B. G.; Furst, E. M. Laser Tweezer Microrheology of a Colloidal Suspension. *J. Rheol.* **2006**, *50* (1), 77−92.
(54) Gurmessa, B.; Fitzpatrick, R.; Falzone, T. T.; Robertson-Anderson, R. M. Entanglement Density Tunes Microscale Nonlinear Response of Entangled Actin. *Macromolecules* **2016**, *49* (10), 3948−3955.
(55) Fitzpatrick, R.; Michieletto, D.; Hauer, C.; Kyrillos, C.; Gurmessa, B. J.; Robertson-Anderson, R. M. Synergistic Interactions between DNA and Actin Trigger Emergent Viscoelastic Behavior. *arXiv:1805.09931 [cond-mat]* **2018**, na.
(56) Mason, T. G.; Weitz, D. A. Optical Measurements of Frequency-Dependent Linear Viscoelastic Moduli of Complex Fluids. *Phys. Rev. Lett.* **1995**, *74* (7), 1250−1253.
(57) Yao, A.; Tassieri, M.; Padgett, M.; Cooper, J. Microrheology with Optical Tweezers. *Lab Chip* **2009**, *9* (17), 2568.
(58) Loosemore, V. E.; Forde, N. R. Effects of Finite and Discrete Sampling and Blur on Microrheology Experiments. *Opt. Express* **2017**, *25* (25), 31239−31252.
(59) Weeks, E.; Crocker, J. M. Particle Tracking Using IDL; http://www.physics.emory.edu/faculty/weeks//idl/.
(60) Tsuda, Y.; Yasutake, H.; Ishijima, A.; Yanagida, T. Torsional Rigidity of Single Actin Filaments and Actin−Actin Bond Breaking Force under Torsion Measured Directly by in Vitro Micromanipulation. *Proc. Natl. Acad. Sci. U. S. A.* **1996**, *93* (23), 12937−12942.
(61) Park, C.-Y.; Jacobson, D. R.; Nguyen, D. T.; Willardson, S.; Saleh, O. A. A Thin Permeable-Membrane Device for Single-Molecule Manipulation. *Rev. Sci. Instrum.* **2016**, *87* (1), 014301.
(62) Gurmessa, B. J.; Bitten, N.; Nguyen, D. T.; Ross, J. L.; Sale, O. A.; Das, M.; Robertson-Anderson, R. M. Active Disassembly and Reassembly of Actin Networks Induces Distinct Biphasic Mechanics. *arXiv:1710.03781 [cond-mat, physics:physics, q-bio]* **2017**, na.
(63) Park, C.-Y.; Jacobson, D. R.; Nguyen, D. T.; Willardson, S.; Saleh, O. A. A Thin Permeable-Membrane Device for Single-Molecule Manipulation. *Rev. Sci. Instrum.* **2016**, *87* (1), 014301.
(64) Nguyen, D. T.; Saleh, O. A. Tuning Phase and Aging of DNA Hydrogels through Molecular Design. *Soft Matter* **2017**, *13* (32), 5421−5427.
(65) Berner, J.; Müller, B.; Gomez-Solano, J.; Krüger, M.; Bechinger, C. Oscillating Modes of Driven Colloids in Overdamped Systems. *Nat. Commun.* **2018**, *9*, 999.
(66) Head, D. A.; Levine, A. J.; MacKintosh, F. C. The Mechanical Response of Semiflexible Networks to Localized Perturbations. *Phys. Rev. E* **2005**, *72* (6), na.
(67) Ronceray, P.; Lenz, M. Connecting Local Active Forces to Macroscopic Stress in Elastic Media. *Soft Matter* **2015**, *11* (8), 1597−1605.

DOI: 10.1021/acsmacrolett.8b00498
ACS Macro Lett. 2018, 7, 968−975